

Transport coefficients near chiral phase transition

Chihiro Sasaki¹ and Krzysztof Redlich^{2,3}

¹*Technische Universität München, D-85748 Garching, Germany*

²*Institute of Theoretical Physics, University of Wrocław, PL-50204 Wrocław, Poland*

³*Institute für Kernphysik, Technische Universität Darmstadt, D-64289 Darmstadt, Germany*
(Dated: June 23, 2018)

We analyze the transport properties of relativistic fluid composed of constituent quarks at finite temperature and density. We focus on the shear and bulk viscosities and study their behavior near chiral phase transition. We model the constituent quark interactions through the Nambu–Jona-Lasinio Lagrangian. The transport coefficients are calculated within kinetic theory under relaxation time approximation including in-medium modification of quasi-particles dispersion relations. We quantify the influence of the order of chiral phase transition and the critical end point on dissipative phenomena in such a medium. Considering the changes of shear and bulk viscosities along the phase boundary we discuss their sensitivity to probe the existence of the critical end point.

PACS numbers: 25.75.Nq, 24.85.+p, 12.39.Fe

1. INTRODUCTION

The shear η and bulk ζ viscosities are parameters that quantify dissipative processes in the hydrodynamic evolution of fluid. Furthermore, it has been argued that ζ and η are sensitive to phase transitions in a medium [1, 2, 3, 4, 5, 6, 7, 8, 9, 10]. Indeed for certain materials, e.g. helium, nitrogen or water, the shear viscosity to entropy ratio η/s is known experimentally to exhibit a minimum at the phase transition [5]. On the other hand, the bulk viscosity ζ/s was argued to be large at the critical point [7, 8, 9, 10].

In QCD of particular interest are properties of transport coefficients near the critical line where deconfinement and chiral phase transition sets in. This is because any change of the bulk and shear viscosities near T_c modifies the hydrodynamic evolution of the QCD medium and influences phenomenological observables that characterize its expansion dynamics.

The recent Lattice Gauge Theory (LGT) calculations in pure SU(3) seem to be consistent with the expectation of decreasing η/s and increasing ζ/s toward the first order deconfinement phase transition approaching from the high temperature phase [11, 12]. The properties of the energy-momentum tensor in the vicinity of the second order phase transition and its importance for the analysis of transport coefficients and their critical behavior have been also calculated and discussed within LGT for (3+1)-dimensional SU(2) gauge theory [13]. All these results show that the transport coefficients are of particular interest to quantify the properties of strongly interacting relativistic fluid and its phase transition [5].

In the theory of critical phenomena, describing dynamical processes near critical point and their universal behavior, the transport coefficients in the second order phase transition can be quantified by a dynamical critical exponents z [14, 15]. These exponents are common for all models belonging to the same dynamical universality class. In general, the critical exponent z determines the critical slowing down of the system relaxation time

$\tau \sim \xi^z \sim |T - T_c|^{-\nu z}$ near the critical temperature T_c with ξ being correlation length and ν its static critical exponent. It was argued that within the classification given by Halperin and Hohenberg the QCD critical end point (CEP) belongs to the universality class of the model H [16]. Consequently, both shear and bulk viscosities are expected to diverge at the CEP as $\eta \simeq \xi^{z_\eta}$ and $\zeta \simeq \xi^{z_\zeta}$ with dynamical critical exponent $z_\eta \simeq 1/19$ and $z_\zeta \simeq 3$ respectively [15].

The analysis of experimental data obtained in heavy ion collisions at RHIC showed that the evolution of the quark gluon plasma (QGP) is well described by nearly ideal hydrodynamics [17]. It has been even argued that the QGP is in fact the most nearly ideal fluid known, with shear viscosity close to the conjectured lower bound in any system [18, 19]. Clearly, in the evolution of QCD medium its transport properties are changing when approaching the phase boundary. Thus, it is of importance to quantify the change of shear and bulk viscosities with thermal parameters near the phase transition expected in strongly interacting medium.

In this paper we explore the transport properties of relativistic fluid composed of constituent quarks at finite temperature and density. The dynamics of medium constituents is described by the chirally invariant four-quark interactions within Nambu–Jona-Lasinio (NJL) model [20, 21]. The model correctly describes the universal critical behavior of physical observables with static critical exponents that belongs to the QCD universality class with respect to chiral symmetry.

To calculate the change of the shear and bulk viscosities with thermal parameters, we assume that the system appears near equilibrium and we apply the kinetic theory under relaxation time approximation [22, 23, 24, 25, 26]. The relaxation time of quarks is obtained from the thermally averaged total cross-section of elastic scattering in the dilute gas approximation [3].

In the NJL model under mean field dynamics the interactions of quarks lead to the quasi-particle description of thermodynamics with their masses $M(T, \mu)$ which are

temperature T - and density μ -dependent [21, 27]. The dynamically generated mass acts as an order parameter for chiral phase transition. In our calculations of transport coefficients, following the method described in Ref. [24], the constituent quark mass $M(T, \mu)$ is consistently built in. We quantify the influence of the order of the chiral phase transition and the critical end point on the shear and bulk viscosities. We show that the bulk viscosity is strongly increasing whereas the shear viscosity is decreasing when approaching the CEP from the side of chirally symmetric phase. These results are consistent with the expectation that the bulk viscosity could dominate dissipative hydrodynamics near CEP [7, 8]. Considering the changes of η and ζ along the phase boundary we discuss their sensitivity to probe the existence of the critical end point.

Within the kinetic theory and under linear response and relaxation time approximation used in this calculation, there is no access to the critical dynamics near second order transition where the properties of shear and bulk viscosities are quantified by dynamical critical exponents. In addition, in this formulation, the transport coefficients are finite with respect to static critical exponents [24]. Thus, the behavior of η and ζ is entirely governed by the non-singular part of the partition function. Consequently, the change of the shear and bulk viscosities with thermal parameters obtained in this paper may depend on specific model dynamics. Nevertheless, one expects that some of our results, e.g. that on the influence of the order of the chiral phase transition on η and ζ , could be relevant for qualitative understanding of transport properties in the QCD medium.

The paper is organized as follows: In Section 2 we introduce the NJL model and its thermodynamics. In Section 3 we describe the methods used to calculate the shear and bulk viscosity. We also quantify in this section the properties of the shear and bulk viscosity near the phase transition and along the phase boundary. Finally, in Section 4 we summarize our results.

2. THE TWO-FLAVOR NJL MODEL

In order to quantify the transport properties of fluid composed of constituent quarks near the chiral phase transition we use the Nambu–Jona-Lasinio (NJL) model [20]. This model exhibits basic properties expected in QCD due to the chiral symmetry restoration. We start with the following Lagrangian for two quark flavors and three colors [21]

$$\mathcal{L} = \bar{\psi}(i\cancel{\partial} - m)\psi + \bar{\psi}\mu\gamma_0\psi + G_S \left[(\bar{\psi}\psi)^2 + (\bar{\psi}i\vec{\tau}\gamma_5\psi)^2 \right], \quad (2.1)$$

where $m = \text{diag}(m_u, m_d)$ and $\mu = \text{diag}(\mu_u, \mu_d)$ are the current quark masses and the quark chemical potentials respectively, whereas $\vec{\tau}$ are Pauli matrices. The coupling of four-fermion interactions $G_S\Lambda^2 = 2.44$ and the three

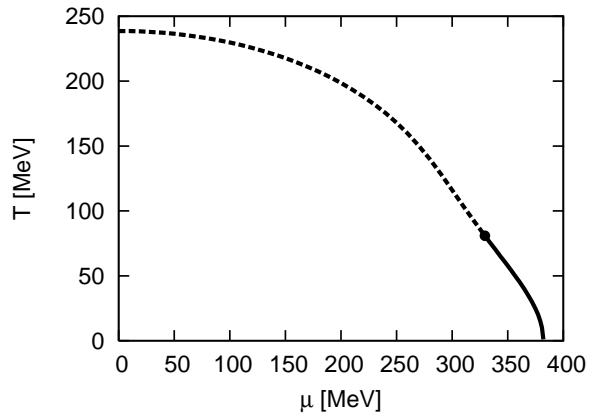


FIG. 1: The phase diagram of the NJL model. The full and dashed lines show the first order and cross over transition respectively. The dot indicates the position of the CEP located at $(T, \mu) = (80.9, 329)$ MeV.

momentum cut-off $\Lambda = 587.9$ MeV are chosen so as to reproduce the vacuum pion decay constant and chiral condensate with $m_u = m_d = 5.6$ MeV.

In the mean field approximation and for the isospin symmetric system the thermodynamics of the NJL model is described by the potential:

$$\Omega(T, \mu; M)/V = \frac{(M - m)^2}{4G_S} - 12 \int \frac{d^3p}{(2\pi)^3} [E(\vec{p}) - T \ln(1 - f(\vec{p}, T, \mu)) - T \ln(1 - \bar{f}(\vec{p}, T, \mu))], \quad (2.2)$$

with $M = m - 2G_S\langle\bar{\psi}\psi\rangle$ being a dynamical quark mass, $E(\vec{p}) = \sqrt{\vec{p}^2 + M^2}$ the quasi-particle energy and $f, \bar{f} = \left(1 + \exp[(E(\vec{p}) \mp \mu)/T]\right)^{-1}$ are the particle/antiparticle distribution functions. The dynamical quark mass M in Eq. (2.2) is obtained self-consistently from the stationarity condition $\partial\Omega/\partial M = 0$ that leads to:

$$M = m + 12G_S \int \frac{d^3p}{(2\pi)^3} \frac{M}{E} [1 - f - \bar{f}]. \quad (2.3)$$

The thermodynamic potential of the NJL model exhibits a typical QCD-like phase diagram shown in Fig. 1. The cross-over transition is identified from the peak position of the chiral susceptibility

$$\chi_{\text{ch}} = -\frac{\partial\langle\bar{\psi}\psi\rangle}{\partial m}. \quad (2.4)$$

The CEP is obtained from the condition of the zero-curvature of an effective potential or equivalently from the divergence of the quark-number susceptibility.

Our main goal is to quantify the transport properties of a medium composed of dynamical quarks with mass $M(T, \mu)$ near the chiral phase transition and along the boundary line shown in the Fig. (1). In this context we explore the shear η and bulk ζ viscosities.

In the thermodynamic system η and ζ are sensitive to thermal and dynamical properties of a medium. To explicitly calculate transport coefficients we use the approach based on the relativistic kinetic theory.

3. TRANSPORT COEFFICIENTS

In the relativistic kinetic theory the transport parameters, the shear and the bulk viscosities, are defined as

$$\eta = \frac{4}{5T} \int \frac{d^3p}{(2\pi)^3} \frac{\vec{p}^4}{E^2} [\tau f(1-f) + \bar{\tau} \bar{f}(1-\bar{f})], \quad (3.1)$$

$$\zeta = -\frac{4}{T} \int \frac{d^3p}{(2\pi)^3} \frac{M^2}{E} \left[(\tau f(1-f) + \bar{\tau} \bar{f}(1-\bar{f})) \left(\frac{p^2}{3E} - \left(\frac{\partial P}{\partial \epsilon} \right)_n \left(E - T \frac{\partial E}{\partial T} - \mu \frac{\partial E}{\partial \mu} \right) + \left(\frac{\partial P}{\partial n} \right)_\epsilon \frac{\partial E}{\partial \mu} \right) - (\tau f(1-f) - \bar{\tau} \bar{f}(1-\bar{f})) \left(\frac{\partial P}{\partial n} \right)_\epsilon \right]. \quad (3.2)$$

The derivatives of pressure P with respect to the net quark number density n or energy density ϵ in Eqs. (3.1) and (3.2) can be expressed in terms of susceptibilities $\chi_{xy} = \partial^2 P / \partial x \partial y$ as

$$\begin{aligned} \left(\frac{\partial P}{\partial \epsilon} \right)_n &= \frac{s\chi_{\mu\mu} - n\chi_{\mu T}}{C_V \chi_{\mu\mu}}, \\ \left(\frac{\partial P}{\partial n} \right)_\epsilon &= \frac{nT\chi_{TT} + (n\mu - sT)\chi_{\mu T} - s\mu\chi_{\mu\mu}}{C_V \chi_{\mu\mu}} \end{aligned} \quad (3.3)$$

with C_V being the specific heat calculated at a constant volume. The C_V is also expressed through susceptibilities

$$C_V = T \left(\frac{\partial s}{\partial T} \right)_V = T \left[\chi_{TT} - \frac{\chi_{\mu T}^2}{\chi_{\mu\mu}} \right]. \quad (3.4)$$

To quantify the change of the above transport coefficients in quasi-particle medium one still needs to specify the relaxation time τ . The τ is calculated from the thermal averaged cross-section describing the total elastic scattering of medium constituents. In the NJL model the medium is composed from constituent quarks with two different flavors. Thus, in the dilute gas approximation the relaxation time τ is obtained from [19, 28]

$$\tau^{-1} = 6 [n_q (\bar{\sigma}_{uu \rightarrow uu} + \bar{\sigma}_{ud \rightarrow ud}) + n_{\bar{q}} (\bar{\sigma}_{u\bar{u} \rightarrow u\bar{u}} + \bar{\sigma}_{u\bar{u} \rightarrow d\bar{d}} + \bar{\sigma}_{u\bar{d} \rightarrow u\bar{d}})], \quad (3.5)$$

where n_i are the quark/antiquark densities

$$\begin{aligned} n_q &= \int \frac{d^3p}{(2\pi)^3} f(p; T, \mu), \\ n_{\bar{q}} &= \int \frac{d^3p}{(2\pi)^3} \bar{f}(p; T, \mu). \end{aligned} \quad (3.6)$$

coefficients of the space-space component of the energy-momentum tensor away from equilibrium.

For the fluid composed of quasi-particles with dynamical mass $M(T, \mu)$ and under the relaxation time approximation, the shear and bulk viscosities are obtained as follows [24]

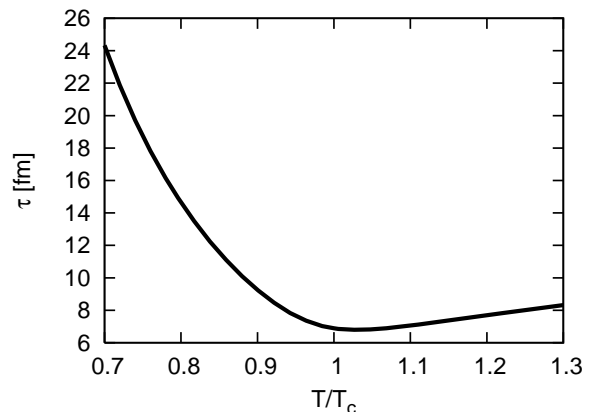


FIG. 2: The collision time in the NJL model at $\mu = 0$.

The in-medium cross section for quark-antiquark, quark-quark and antiquark-antiquark scattering processes were studied in detail in Ref. [3] including $1/N_c$ next to leading order corrections. For $u\bar{u} \rightarrow u\bar{u}$ scattering the differential cross section is obtained from the T matrix as

$$\begin{aligned} &\frac{d\sigma_{u\bar{u} \rightarrow u\bar{u}}(s, t; T, \mu)}{dt} \\ &= \frac{1}{16\pi s(s - 4M^2)} \sum_{c,s} |T_{u\bar{u} \rightarrow u\bar{u}}|^2(s, t; T, \mu), \end{aligned} \quad (3.7)$$

where the average over the initial color and spin as well as the summation over final states were taken. We consider the rest frame of colliding quarks so that the differential cross section (3.7) is expressed as the function of

the Mandelstam variables s and t . The integrated cross section is calculated from

$$\begin{aligned} \sigma_{u\bar{u}\rightarrow u\bar{u}}(s; T, \mu) &= \int dt \frac{d\sigma_{u\bar{u}\rightarrow u\bar{u}}}{dt} \frac{-4t(s+t-4M^2)}{(s-4M^2)^2} \\ &\times (1 - f(\sqrt{s}/2 - \mu)) (1 - \bar{f}(\sqrt{s}/2 + \mu)). \end{aligned} \quad (3.8)$$

In the above equation we have taken into account that the transport process is dominated by the large angle scattering [28]. The terms in the brackets correspond to the Pauli blocking factors which account for a possible occupation of particles in the final state. We also introduce the energy-averaged cross section

$$\bar{\sigma}_{u\bar{u}\rightarrow u\bar{u}}(T, \mu) = \int ds \sigma_{u\bar{u}\rightarrow u\bar{u}}(s; T, \mu) P(s; T, \mu), \quad (3.9)$$

with P being the probability of yielding $q\bar{q}$ pair with the energy s

$$\begin{aligned} P(s; T, \mu) &= C \sqrt{s(s-4M^2)} \\ &\times f(\sqrt{s}/2 - \mu) \bar{f}(\sqrt{s}/2 + \mu) v_{\text{rel}}(s), \end{aligned} \quad (3.10)$$

where the relative velocity between two particles in the initial state v_{rel} is given by

$$v_{\text{rel}}(s) = \sqrt{\frac{s-4M^2}{s}}. \quad (3.11)$$

The normalization constant C is fixed from

$$\int ds P(s; T, \mu) = 1. \quad (3.12)$$

The differential cross sections for different quark flavors are obtained through the isospin symmetry, charge conjugation and crossing symmetry. The total cross section after the energy averaging reads

$$\bar{\sigma}_q = \bar{\sigma}_{u\bar{u}\rightarrow u\bar{u}} + \bar{\sigma}_{u\bar{u}\rightarrow d\bar{d}} + \bar{\sigma}_{u\bar{d}\rightarrow u\bar{d}} + \bar{\sigma}_{uu\rightarrow uu} + \bar{\sigma}_{ud\rightarrow ud}. \quad (3.13)$$

The dominant contribution to the total cross section (3.13) comes from the s-channel due to the propagation of π and σ modes. The mass of σ drops toward the critical temperature T_c and due to chiral symmetry restoration is degenerated with the pion mass at $T = T_c$. On the other hand, for $T > T_c$, both π and σ masses are increasing with temperature. Consequently, the cross section $\sigma(s = m_\sigma^2; T, \mu)$ shows singularity at T_c [3] ^{#1}. However, after the integration over energy s this singularity is mostly washed out in the total cross section $\bar{\sigma}_q$. As remnants of the above singularity a broad bump in the $\bar{\sigma}_q$ is seen around T_c [3]. Thus, the total cross section is non-singular even at the CEP.

Fig. 2 shows the collision time calculated from Eq. (3.1) at finite T and at $\mu = 0$. There is a clear decrease of τ when approaching the critical region from the chirally broken phase. One should realize that in spite of the phase transition the collision time is quite smooth around T_c and experiences only a shallow minimum at the phase transition. This behavior is due to the total cross section which shows a similar broad structure around T_c . The τ is large at low and small at high temperatures since the quark density is increasing function of temperature ^{#2}.

At the finite μ the total cross-section is larger than that at $\mu = 0$ and the quark density increases while the anti-quark density decreases. Consequently, the collision time for quark τ and for anti-quark $\bar{\tau}$ behaves as

$$\tau(\mu) > \tau(\mu = 0), \quad \bar{\tau}(\mu) < \bar{\tau}(\mu = 0). \quad (3.14)$$

With the above results for the collision time applied in Eq. (3.1) we can calculate the transport coefficients in the quasi-quark medium and study their sensitivity to the chiral phase transition.

3.1. Bulk and shear viscosities near phase transition

The temperature and density dependence of the shear viscosity obtained in the NJL model under relaxation time approximation is shown in Fig. 3. For low density the shear viscosity shows a shallow minimum near the pseudo-critical temperature. This behavior is similar as that observed in the collision time. The constituent quark mass decreases with temperature and the quark density is enhanced in the chirally symmetric phase which results in the rise of η at high temperature. Quantitatively the difference in η at $\mu = 0$ and $\mu \neq 0$ comes mainly from the density effect. Consequently, at the CEP and near the first-order phase transition, this effect should be even more significant. Fig. 3-(right) shows the change of shear viscosity when crossing the CEP and the boundary of the first order phase transition. As expected, the η shows discontinuity at the first order transition. At the CEP this discontinuity disappears, however there is still an abrupt change of η . One observes that the shear viscosity is decreasing toward the CEP and first order phase transition from the side of the symmetric phase.

When discussing the transport properties of relativistic fluid a natural normalization of shear viscosity is the entropy density s . In this way the η/s is dimensionless quantity that characterizes dissipation of energy in a medium. Fig. 4 shows the temperature dependence of the ratio η/s at vanishing and at finite chemical potential. The entropy density rapidly increases with temperature,

^{#1} More precisely, the singularity appears at the pionic Mott temperature at which the pion mass becomes equal to the mass of its constituents, $m_\pi = 2M$. In the chiral limit the Mott temperature coincides with the chiral phase transition temperature.

^{#2} The behavior of τ at $T \ll T_c$ seen in Fig. 2 is specific for the NJL model where in the low-temperature phase the medium is composed only of heavy constituent quarks.

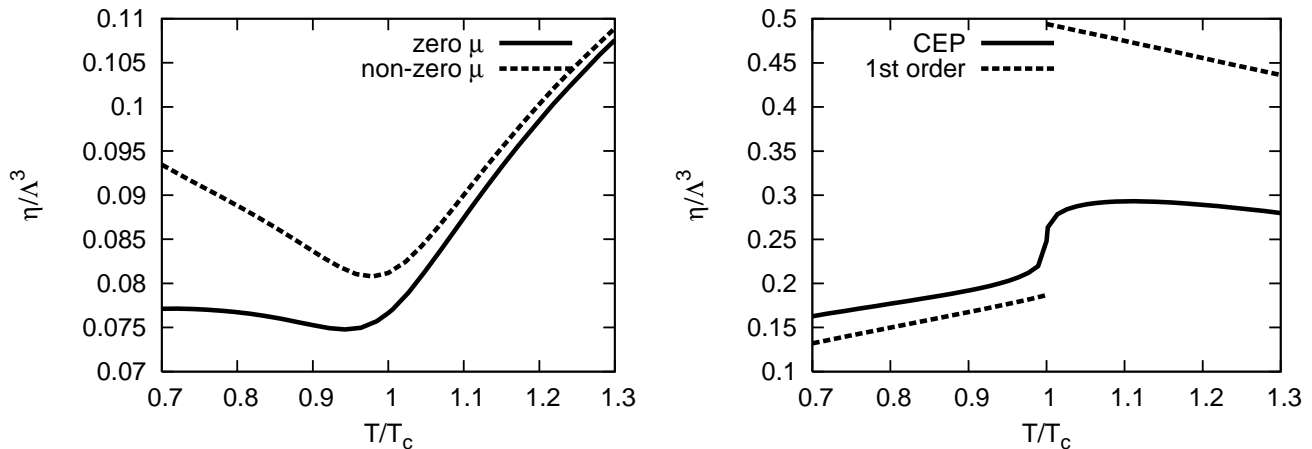


FIG. 3: The shear viscosity normalized by the 3-momentum cutoff around cross over (left-hand figure) and around μ_{CEP} and first order transition (right-hand figure).

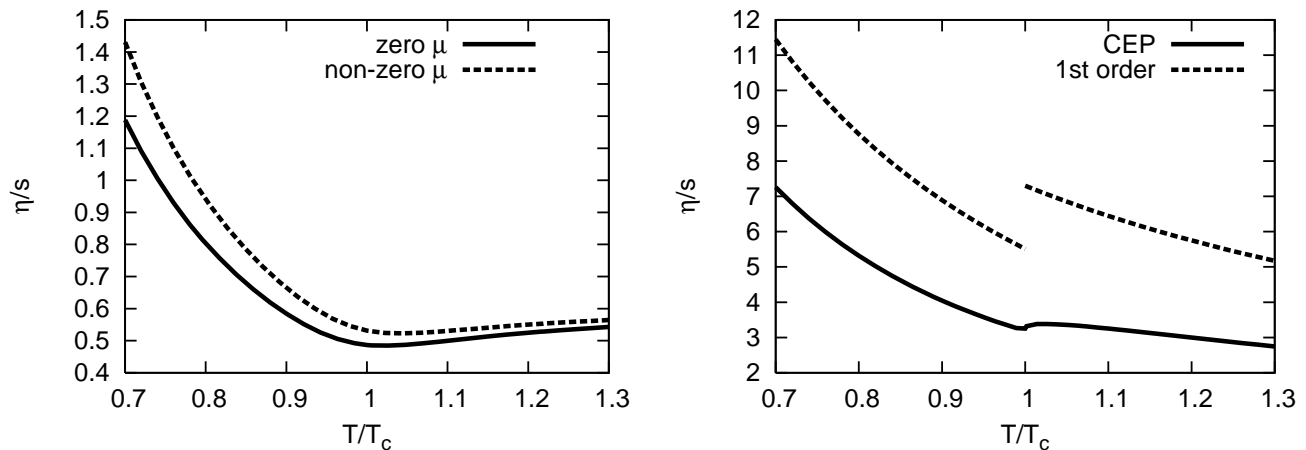


FIG. 4: The ratio of shear viscosity to entropy density around cross over (left-hand figure) and around μ_{CEP} and first order transition (right-hand figure).

thus the η/s is reduced in the high-temperature phase. A shallow minimum structure around T_c for small μ is not preserved with increasing μ . From Fig. 4-(right) one sees that η/s is insensitive to the existence of the CEP. At higher μ the ratio shows a jump associated with the first order phase transition.

From the general analytic expression for the shear and the bulk viscosities (see Eqs. (3.2) and (3.1)) one expects that ζ should be more sensitive to the phase transition than η due to explicit contribution of derivative terms involving a dynamical quark mass. Fig. 5 shows the temperature dependence of ζ for different μ . In the regime of cross-over transition the density dependence of ζ is much weaker than that seen in the shear viscosity. This is indeed due to $\partial M/\partial T$ and $\partial M/\partial \mu$ terms that contribute to the bulk and are absent in the shear viscosity. The temperature dependence of ζ at finite μ is similar to that

at $\mu = 0$ as seen in Fig. 5-(left). With the increasing chemical potential, the quark density effects start to be visible. The growth of ζ toward T_c in Fig. 5-(right) is due to an increase of quark number density. At the CEP the bulk viscosity is finite in spite of the fact that all susceptibilities contributing to ζ are diverging [24]. Thus, at the CEP there is a precise cancellation of singularities from different terms in Eq. (3.2). Nevertheless, one observes a rapid downward change approaching the CEP from the low-temperature side. This reflects the change of the dynamical quark mass with temperature.

The ratio ζ/s , of the bulk viscosity to the entropy density, keeps basically a structure of ζ/Λ^3 . The suppressed entropy density due to the heavy constituent quark mass in low-temperature phase results in growth of the ratio shown in Fig. 6. The rate of change in ζ/s with temperature at CEP is higher than that of η/s . However,

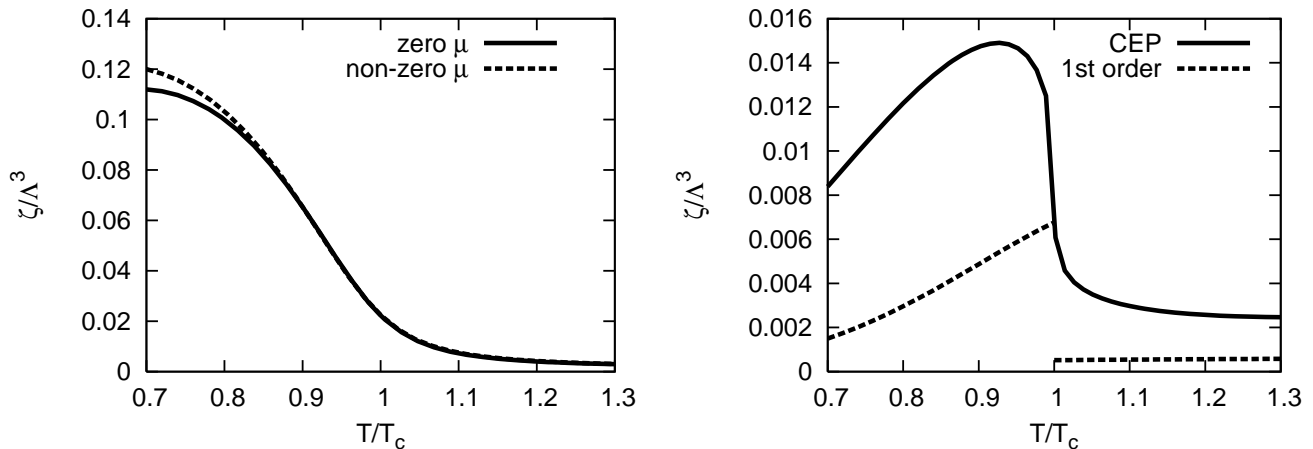


FIG. 5: The bulk viscosity normalized by the 3-momentum cutoff around the cross over (left-hand figure) and around μ_{CEP} and first order transition (right-hand figure).

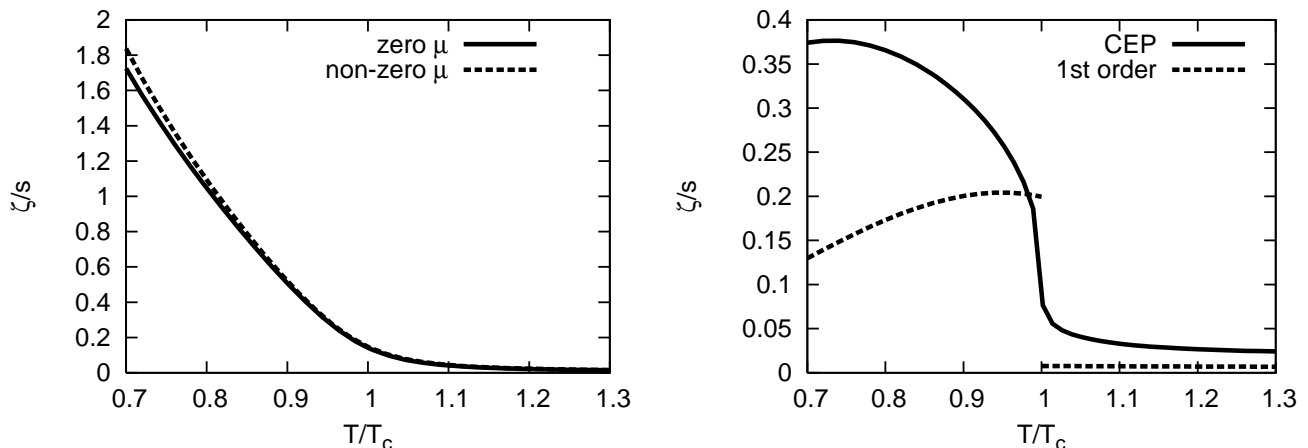


FIG. 6: The ratio of bulk viscosity to entropy density around the cross over (left-hand figure) and around μ_{CEP} and first order transition (right-hand figure).

the absolute value of ζ/s is smaller than η/s at CEP. This result is valid under relaxation time approximation where τ is always finite. However, when going beyond this approximation and including dynamical scaling [15], the bulk viscosity should be singular at the CEP.

In the derivation of the bulk viscosity we have explicitly included in Eq. (3.2) the modification of particle dispersion relations due to a dynamically generated quasi-particle mass which is T and μ dependent. In Fig. 7 we quantify the influence of derivatives of a dynamical mass on the bulk viscosity. The full-line in this figure was obtained from Eq. (3.2) whereas the dashed-line was calculated by eliminating the $\partial M/\partial T$ and $\partial M/\partial \mu$ terms from Eq. (3.2). The behavior of ζ is largely governed by the dynamical quark mass $M(T, \mu)$ multiplied in front of (3.2). Unlike the expectation that the bulk viscosity should be sensitive to the phase transition, there is no

much difference in the above two cases. The enhancement of $\partial M/\partial T$ around T_c is weakened by the pre-factor M^2 in Eq. (3.2). In addition, the contributions of different susceptibilities in Eq. (3.2) which are diverging at the CEP are canceled out, leading to a finite bulk viscosity at the critical end point [24].

The NJL model, being non-renormalizable, requires the ultraviolet momentum cut-off Λ . Consequently, all thermodynamic quantities are affected by finite Λ . This is particularly the case in the parameter range where the physics is sensitive to a large particle momenta. Fig. 8 shows sensitivity of η/s and ζ/s to the momentum cut-off Λ_T implemented in the thermal part of thermodynamic potential. We compare the results obtained with $\Lambda_T = \Lambda_{T=0} = 587.9$ MeV and with $\Lambda_T=1$ GeV. In high temperature phase we also show in Fig. 8 the resulting viscosities obtained from the perturbative QCD

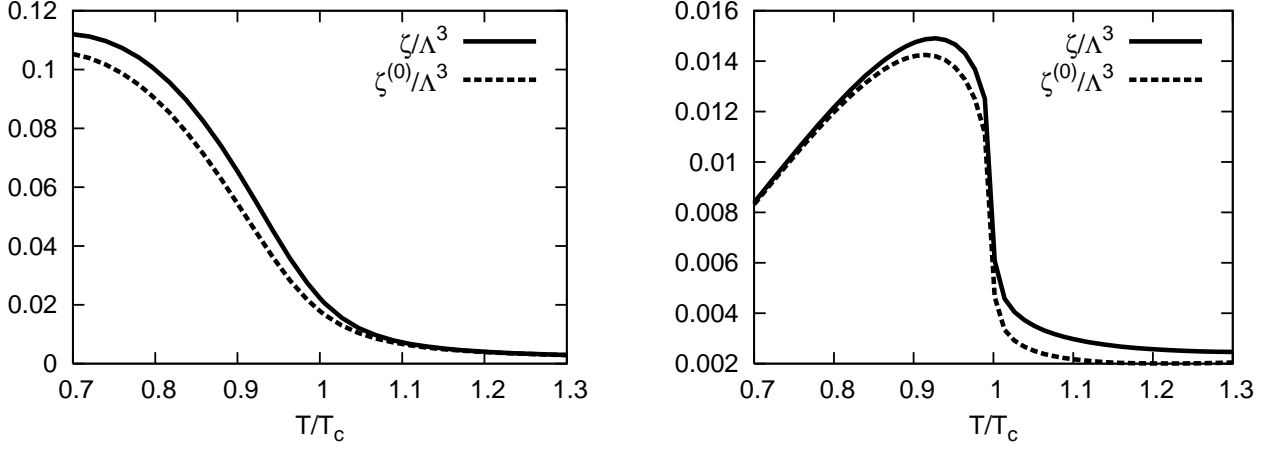


FIG. 7: The bulk viscosity normalized by the 3-momentum cutoff at $\mu = 0$ (left-hand figure) and at μ_{CEP} (right-hand figure). The solid line is obtained from Eq. (3.2) whereas the dashed line from the same equation after eliminating the terms proportional to mass derivatives.

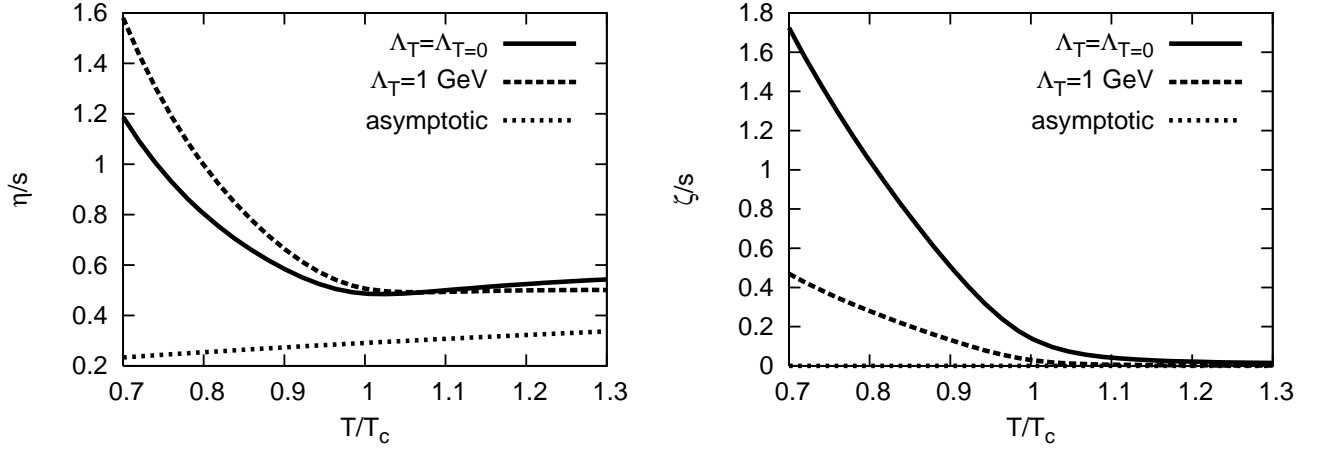


FIG. 8: The ratio of η/s (left-hand figure) and ζ/s (right-hand figure) at $\mu = 0$. The solid curves are obtained with the same 3-momentum cutoff Λ_T in thermal part as in the vacuum, i.e., $\Lambda_T = 587.9 \text{ MeV}$. The dashed lines are obtained for $\Lambda_T = 1 \text{ GeV}$ in thermal part while in vacuum part $\Lambda = 587.9 \text{ MeV}$ is used. The dotted curves indicate the asymptotic values for massless quarks in high temperature limit.

(pQCD) [22] ^{#3}

$$\begin{aligned} \eta^{(\text{asymptotic})} &= \frac{4\pi^2}{675} \frac{3.86}{\alpha_s^2 \ln(1/\alpha_s)} T^3, \\ \zeta^{(\text{asymptotic})} &= 0, \end{aligned} \quad (3.15)$$

with the two-loop running coupling for $N_f = 2$

$$\alpha_s = 2\pi \left[\frac{29}{3} \ln(T/\lambda) + \frac{115}{29} \ln(2 \ln(T/\lambda)) \right]^{-1}, \quad (3.16)$$

and with $\lambda = 30 \text{ MeV}$.

As seen in Fig. 8, both η/s and ζ/s are very sensitive to the momentum cut-off. However, at low T this dependence is opposite in shear and bulk viscosity. There is an increase of η/s and decrease of ζ/s with increasing Λ . This is due to derivative terms in the bulk viscosity which show steeper change with Λ . At high temperature the NJL model results tend to converge to that expected in pQCD. The bulk viscosity vanishes at high temperature, as expected in the conformal theory. However, due to the absence of gluons and the presence of the finite cut-off the shear viscosity deviates from their asymptotic value even at $T \gg T_c$.

^{#3} For the recent results of viscosity parameters obtained in the high temperature QCD see Ref. [25].

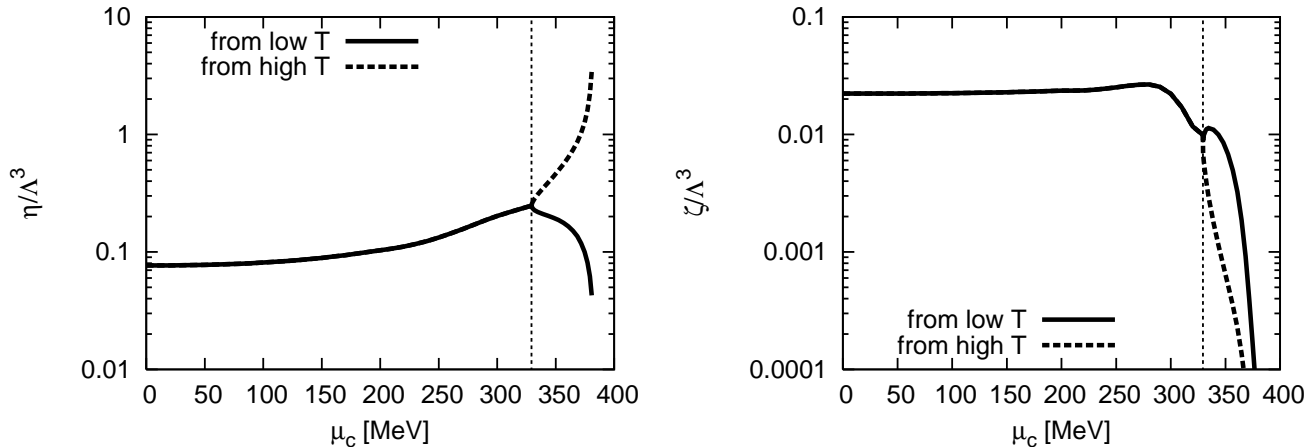


FIG. 9: The shear (left-hand figure) and bulk (right-hand figure) viscosities normalized by the 3-momentum cutoff calculated along the phase boundary. The vertical dotted-line indicates the position of the CEP.

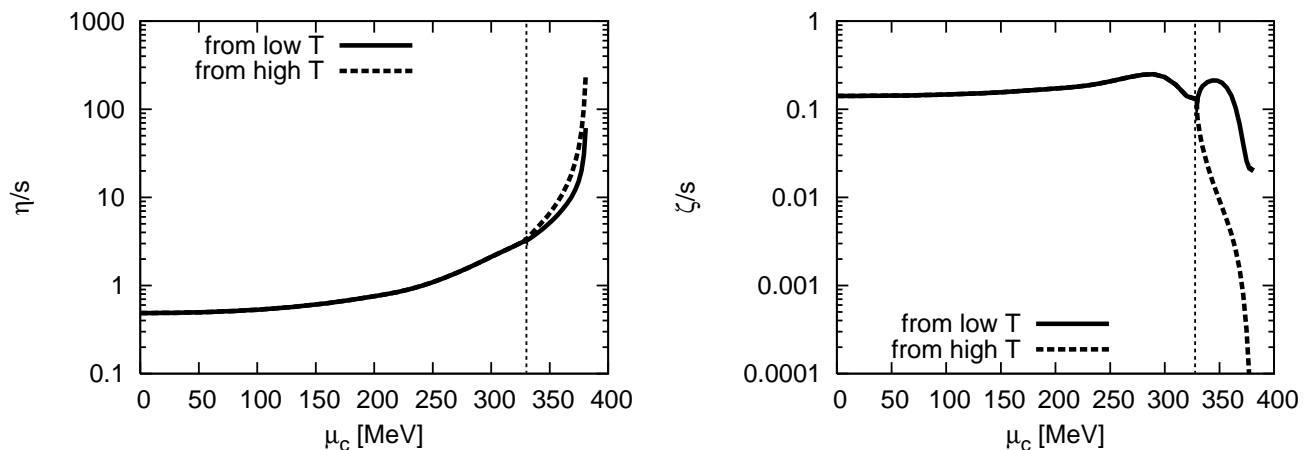


FIG. 10: The ratio of shear (left-hand figure) and bulk (right-hand figure) viscosities to entropy density calculated along the phase boundary. The vertical dotted-line indicates the position of the CEP.

3.2. Viscosities along the phase boundary

Fig. 9 shows the shear and bulk viscosities calculated along the chiral phase boundary obtained in the NJL model and shown in Fig. 1. Two lines at high μ_c indicate a gap associated with the first order transition. The shear viscosity increases along the cross-over line towards the CEP where it reaches its maximal value. The bulk viscosity is rather weakly changing with T in the regime of cross-over and exhibits a local minimum at the CEP. A little bump on the cross-over line before reaching the CEP is an artifact of the present NJL model calculation. In a more realistic calculation, this may disappear and the bulk viscosity smoothly goes down to the CEP. The η shows an upward jump approaching the first order transition from the low-temperature phase. This is an opposite behavior to ζ which shows a downward jump.

Fig. 10 shows the ratios, η/s and ζ/s , calculated along the critical line. The η/s is monotonic along the critical line without showing any sensitivity to the CEP. The ζ/s preserves the local minimum at the CEP and shows a visible gap at the first order transition.

The properties of the transport coefficients calculated within NJL model are not universal in spite of the fact that this model belongs to the QCD universality class with respect to chiral symmetry. In addition the shear and bulk viscosities are sensitive to particle composition of the medium and to specific model dynamics that enters to various collision processes. The shear and bulk viscosities do not show critical behavior with static critical exponents. Nevertheless, one expects that some generic features of transport coefficients along the phase boundary calculated within the above model could be of interest for understanding transport properties of the QCD matter.

From this perspective, a trace of in-medium change of the order parameter $M(T, \mu)$ remains more distinctly in the bulk than in the shear viscosity.

4. SUMMARY AND CONCLUSIONS

Based on the NJL model and kinetic theory we have shown the transport properties of thermal medium composed of dynamical quarks. We have included in our calculations in-medium modification of constituent quark dispersion relations. We have analyzed behaviors of shear η and bulk ζ viscosities near the chiral phase transition within the mean field approximation. The collision time required to quantify viscosity parameters was calculated from the elastic scattering cross-section of constituent quarks including next to leading $1/N_c$ corrections.

We have shown that around the phase transition the shear viscosity exhibits only a shallow minimum for small chemical potentials. For higher μ corresponding to the first order transition and near the critical end point the shear viscosity is discontinuous or exhibits an abrupt change. However, when normalizing η by the entropy density s this abrupt change at CEP disappears. The bulk viscosity is more sensitive to the change of the dynamical quark mass around the phase transition, thus shows steeper behavior near T_c , however stays non-

singular at CEP.

Along the chiral phase boundary the η/s is changing monotonically with critical parameters whereas the ζ/s has a local minimum at the CEP. Nevertheless, within the considered model and under relaxation time approximations none of viscosities could be considered as a useful probe of the critical end point in the phase diagram. We have to stress that due to the non-universal behavior of bulk and shear viscosity within these calculations our quantitative results are model dependent. However, we expect that qualitative behavior of η/s and ζ/s near the chiral phase boundary derived here could be less sensitive to the specific model dynamics since important change of the order parameter is certainly incorporated in our formula.

Acknowledgments

We acknowledge interesting discussions with B. Friman and J. Wambach. C.S. acknowledges partial support by the DFG cluster of excellence "Origin and Structure of the Universe". K.R. acknowledges partial support of the Polish Ministry of Science and Higher Education (MENiSW) and the Deutsche Forschungsgemeinschaft (DFG) under the "Mercator program".

-
- [1] J. Kapusta, Phys. Rev. C **24**, 2545 (1981). M. Prakash, M. Prakash, R. Venugopalan and G. Welke, Phys. Rept. **227**, 321 (1993). P. Kovtun, D. T. Son and A. O. Starinets, Phys. Rev. Lett. **94**, 111601 (2005). T. Hirano and M. Gyulassy, Nucl. Phys. A **769**, 71 (2006). P. Romatschke and U. Romatschke, Phys. Rev. Lett. **99**, 172301 (2007). A. Muronga, Phys. Rev. C **76**, 014909 (2007); Phys. Rev. C **76**, 014910 (2007). K. Dusling and D. Teaney, Phys. Rev. C **77**, 034905 (2008). H. Song and U. W. Heinz, Phys. Lett. B **658**, 279 (2008). G. Torrieri, B. Tomasik and I. Mishustin, Phys. Rev. C **77**, 034903 (2008).
- [2] J. I. Kapusta, arXiv:0809.3746 [nucl-th].
- [3] P. Zhuang, J. Hufner, S. P. Klevansky and L. Neise, Phys. Rev. D **51**, 3728 (1995). P. Rehberg, S. P. Klevansky and J. Hufner, Nucl. Phys. A **608**, 356 (1996).
- [4] A. Dobado and F. J. Llanes-Estrada, Phys. Rev. D **69**, 116004 (2004). J. W. Chen, Y. H. Li, Y. F. Liu and E. Nakano, Phys. Rev. D **76**, 114011 (2007). P. Czerski, W. M. Alberico, S. Chiacchiera, A. De Pace, H. Hansen, A. Molinari and M. Nardi, arXiv:0708.0174 [hep-ph]. K. Itakura, O. Morimatsu and H. Otomo, Phys. Rev. D **77**, 014014 (2008).
- [5] L. P. Csernai, J. I. Kapusta and L. D. McLerran, Phys. Rev. Lett. **97**, 152303 (2006).
- [6] R. A. Lacey *et al.*, Phys. Rev. Lett. **98**, 092301 (2007).
- [7] K. Paech and S. Pratt, Phys. Rev. C **74**, 014901 (2006).
- [8] D. Kharzeev and K. Tuchin, arXiv:0705.4280 [hep-ph].
- [9] A. M. Polyakov, JETP **57**, 2144 (1969).
- [10] F. Karsch, D. Kharzeev and K. Tuchin, Phys. Lett. B **663**, 217 (2008).
- [11] A. Nakamura and S. Sakai, Phys. Rev. Lett. **94**, 072305 (2005). H. B. Meyer, Phys. Rev. D **76**, 101701 (2007).
- [12] H. B. Meyer, Phys. Rev. Lett. **100**, 162001 (2008).
- [13] K. Huebner, F. Karsch and C. Pica, Phys. Rev. D **78**, 094501 (2008).
- [14] P. C. Hohenberg and B. I. Halperin, Rev. Mod. Phys. **49**, 435 (1977).
- [15] A. Onuki, *Phase Transition Dynamics* (Cambridge University Press, 2002), p. 277.
- [16] D. T. Son and M. A. Stephanov, Phys. Rev. D **70**, 056001 (2004).
- [17] D. Teaney, J. Lauret and E. V. Shuryak, Phys. Rev. Lett. **86** 4783 (2001). P. Huovinen, P. F. Kolb, U. W. Heinz, P. V. Ruuskanen and S. A. Voloshin, Phys. Lett. B **503**, 58 (2001). E. V. Shuryak, Nucl. Phys. A **750**, 64 (2005). M. Gyulassy and L. McLerran, Nucl. Phys. A **750**, 30 (2005).
- [18] P. Kovtun, D. T. Son and A. O. Starinets, JHEP **0310**, 064 (2003); Phys. Rev. Lett. **94** 111601 (2005).
- [19] P. Danielewicz and M. Gyulassy, Phys. Rev. D **31**, 53 (1985).
- [20] Y. Nambu and G. Jona-Lasinio, Phys. Rev. **122**, 345 (1961); Phys. Rev. **124**, 246 (1961).
- [21] For reviews and applications of the NJL model to hadron physics, see e.g., U. Vogl and W. Weise, Prog. Part. Nucl. Phys. **27**, 195 (1991). S. P. Klevansky, Rev. Mod. Phys. **64** (1992) 649. T. Hatsuda and T. Kunihiro, Phys. Rept. **247**, 221 (1994). M. Buballa, Phys. Rept. **407**, 205 (2005).

- [22] A. Hosoya and K. Kajantie, Nucl. Phys. B **250**, 666 (1985).
- [23] S. Gavin, Nucl. Phys. A **435**, 826 (1985).
- [24] C. Sasaki and K. Redlich, arXiv:0806.4745 [hep-ph].
- [25] P. Arnold, C. Dogan and G. D. Moore, Phys. Rev. D **74**, 085021 (2006).
- [26] G. D. Moore and O. Saremi, arXiv:0805.4201 [hep-ph].
- [27] C. Sasaki, B. Friman and K. Redlich, Phys. Rev. D **75**, 054026 (2007); Phys. Rev. D **77**, 034024 (2008).
- [28] F. Reif, *Fundamentals of Statistical and Thermal Physics* (McGraw-Hill, New York, 1965).